# New Dynamical Aspects of the Driven Pendulum

Noboru TAKIMOTO and Masatoshi TANGE
Department of Engineering Science, Tohoku University, Sendai 980

The driven pendulum is studied numerically and analytically under off-resonance condition, where the driving frequency $\omega$ is larger than the linear characteristic frequency $\omega_0$ of the pendulum. As is well known, a symmetry-breaking occurs when the driving amplitude $f$ exceeds a critical value $f_c$, but further increase of $f$ does not lead to a chaos, but to an inversion of the pendulum. It is also shown that four stationary states coexist for intermediate values of $f$. Most of the results obtained numerically can be explained by perturbation expansion solutions of the equation of motion.

**§1. Introduction.** The driven pendulum has been studied in the context of the deterministic chaos, including normal or anomalous diffusion.[1)−6)] The dynamical structures that have been established so far are as follows. We denote the angular coordinate of the pendulum by $x$, and consider only a sinusoidal driving force $f\cos\omega t$. In most previous works, $\omega$ has been smaller than $\omega_0$. Since the characteristic frequency of this particular system decreases because of non-linear effect, the driving force in this case is always in near resonance with the oscillatory motion of the pendulum. A general non-chaotic motion is a rotary oscillation, which combines an oscillation with a phase-locked rotation, characterized by an integer $n$, which counts the number of rotations per period $2\pi/\omega$. The time average $<\dot{x}>$ of $\dot{x}$ in state $n$ is thus $n\omega$. For small $f$ only pure rotations ($n=0$) occur. When $f$ exceeds $f_c$, there occurs a symmetry-breaking, which for further increase of $f$ leads to cascading subharmonic bifurcations, and finally to chaos.

It appears that nothing remains to be studied concerning the driven pendulum. To our knowledge, however, a few interesting aspects have been overlooked. They are observed not in the chaotic but in the pre-chaotic phase, where $\omega$ is larger than $\omega_0$. In this paper we shall study the driven pendulum under such an off-resonance condition.

**§2. The numerical integrations.** The equation of motion of the driven pendulum is

$$\mathrm{D}^2x + 2\lambda\mathrm{D}x + \sin x = f\cos\omega t, \tag{2.1}$$

where D is the operator $\mathrm{d}/\mathrm{d}t$, $\lambda$ the damping constant and $\omega_0$ is normalized to unity. If $x$ is a solution, then $x+2\pi N$ with $N$ an arbitrary integer is also a solution, but in the following

we shall regard them identical. The conventional stationary solution takes the form

$$x = A_1 \cos\theta_1 + A_3 \cos\theta_3 + A_5 \cos\theta_5 + \cdots, \theta_m = m\omega t - \alpha_m \ (A_m > 0,\ 0 < \alpha_m < \pi),$$

and will be called the normal state. The system (2.1) has three parameters $\lambda, \omega$ and $f$, and these together with the two initial conditions constitute the system parameters. We take $f > 0$ for definiteness, and are interested in the case $\omega = 2$ and $\lambda = 0.1$, where higher harmonics are almost completely negligible.

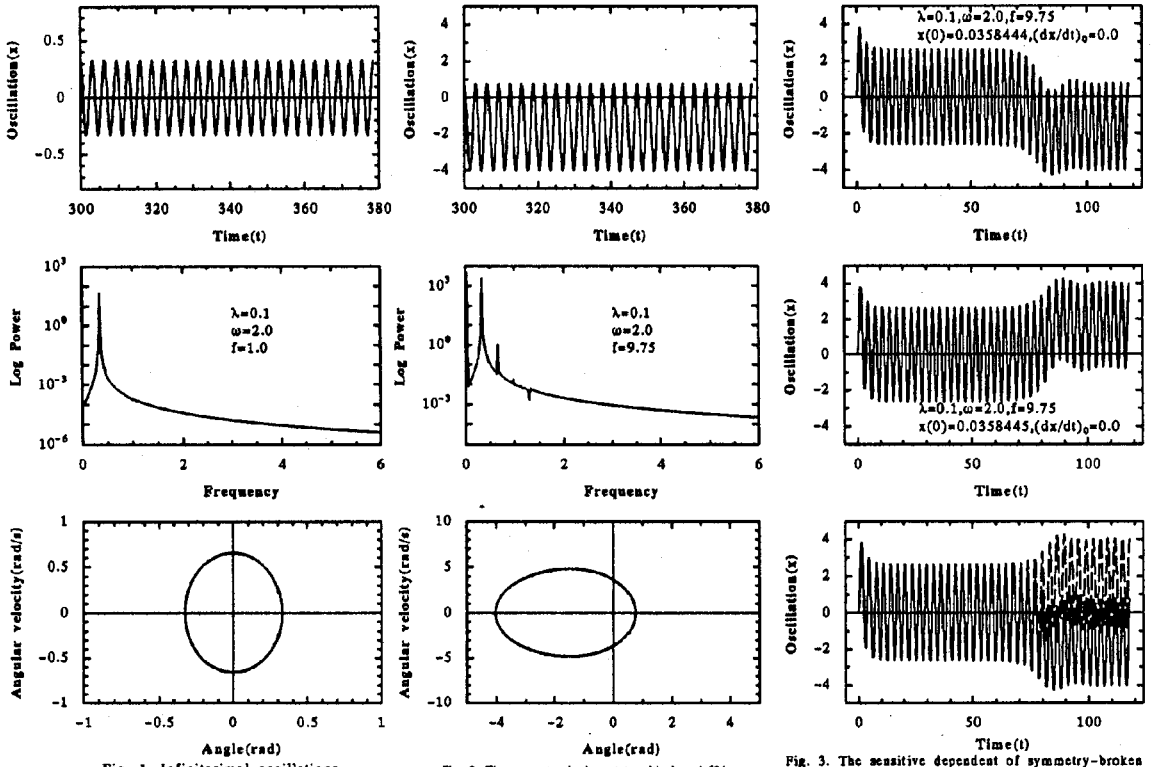


Fig. 1. Infinitesimal oscillations.

Fig. 2. The symmetry-broken state with $A_z \sim -1.634$.

Fig. 3. The sensitive dependent of symmetry-broken states on the initial conditions. The first two waves forms are superposed in the last figure.

The numerical integration is based on the fourth order Runge-Kutter method with double precision, in which the time increment $h$ is taken to be 0.01, but when the analysis gets involved, we let $h = 0.001$. Unless otherwise stated, we start with the initial conditions $(x(0), \dot{x}(0)) = (0, 0)$, and discard all data between $t = 0$ and $t = 30/\lambda$ as representing the transient effects. The wave form $x(t)$ for $f = 1$ is shown in Fig.1 together with its power spectrum. On the bottom of the figure is drawn a trajectory in phase space. As $f$ increases, $A_1$ also increases, and the dynamics of the driven pendulum change in the following way. If $f$ exceeds $f_c \sim 8.77$, $A_1$ exceeds $A_c \sim 2.425$, and the stationary solution takes the form $x = A_0 + A_1 \cos\theta_1 + A_2 \cos\theta_2 + A_3 \cos\theta_3 + \cdots$; i.e., there occurs a symmetry-breaking, accompanied by even harmonics. The value 2.425 is approximately the first zero $A_z$ of

the Bessel function $J_0(A_1)$. The appearance of $J_0$ is based on the analytic integration to be carried out in §3. Fig.2 shows an example at this stage. The sign of $A_0$ depends on the system parameters, and sometimes this dependence is very sharp. For $f = 9.75$ and $h = 10^{-3}$ we find $A_0 = -1.6335514$ for the initial conditions (0.0358444,0), but $A_0 = 1.6335514$ for (0.0358445,0). Fig.3 shows two waves, starting with almost the same initial conditions, yet leading to different signs of $A_0$. In other words, the motion is unstable at this value of $x(0)$, in contrast with a chaos unstable almost everywhere in a definite region of phase space.

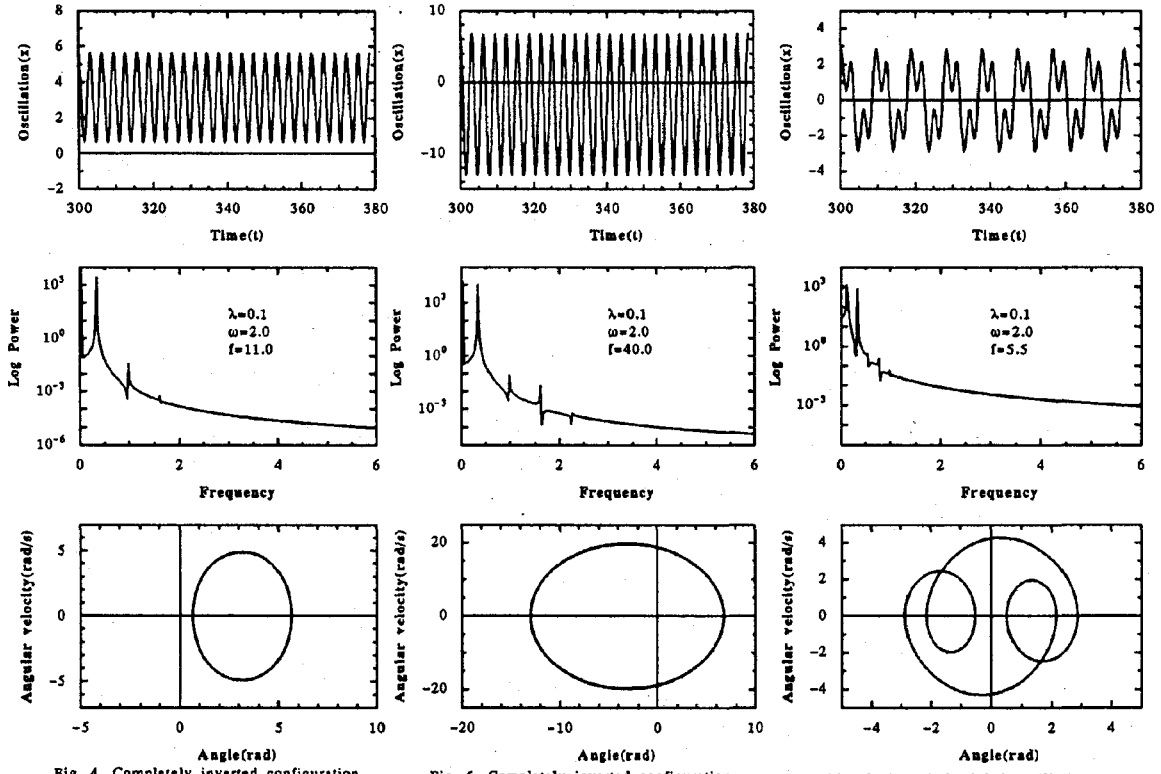


Fig. 4. Completely inverted configuration.

Fig. 5. Completely inverted configuration in the second stage

Fig. 6. A period-tripled oscillation.

After symmetry is broken, $|A_0|$ increases, while $A_1$ is kept at $A_z$. For $\omega$ less than unity, as in most previous works, a series of period-doubling bifurcations and finally a chaos occur, before $|A_0|$ reaches $\pi$. On the other hand, for larger $\omega$ as in our case, $|A_0|$ reaches $\pi$ at $f \sim 10.58$, where the pendulum oscillates in the inverted configuration! When $f$ further increases, $A_1$ increases, while $|A_0|$ is kept exactly at $\pi$, until $A_1$ reaches the second zero $A_z' \sim 5.43$ of $J_0$. This stage of motion is shown in Fig.4. After that, $|A_0|$ decreases with $A_1$ kept at $A_z'$, until $A_0$ goes to zero, or the pendulum returns to the normal configuration. Then $A_1$ increases in the normal configuration, until it reaches the third zero $\sim 8.65$ of $J_0$. Further increase of $f$ leads to a second symmetry-breaking, and so on. Fig.5 shows an inverted

configuration in the second stage. It is remarkable that even at this stage higher harmonics are still quite negligible.

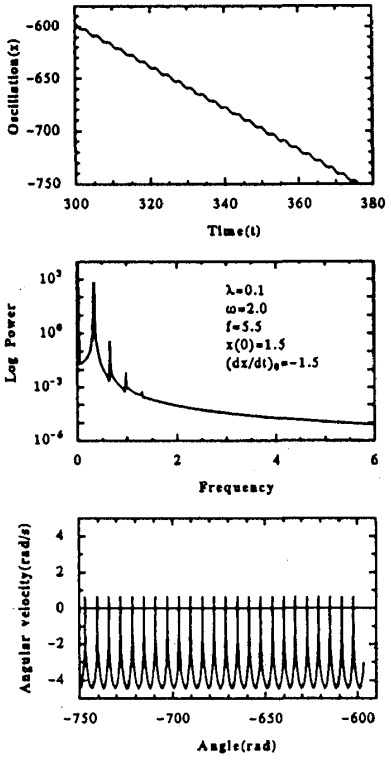


Fig. 7. A sinusoidally modulated rotation in the negative direction

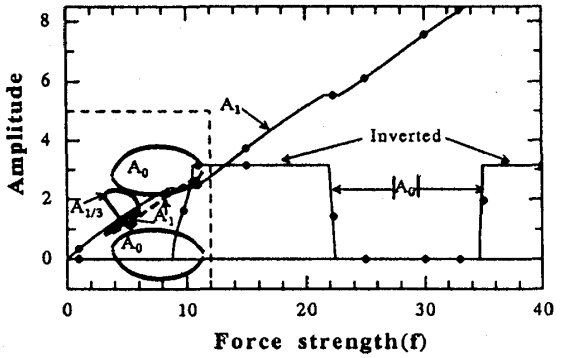


Fig. 8. The overall view of the dynamical structures.

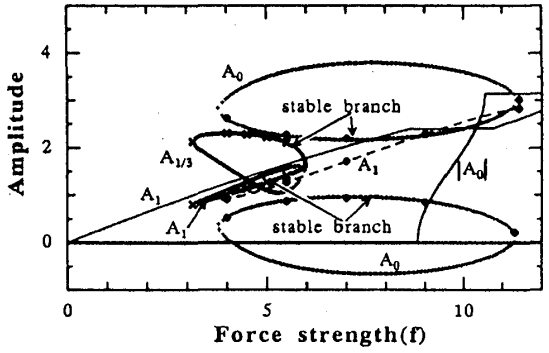


Fig. 9. The overall view of the dynamical structures in which the four phases are emphasized.

In the range $f \in [3.16, 5.97]$ appears a period-tripled state, described by $x = A_1 \cos\theta_1 + A_{1/3} \cos\theta_{1/3}$, and in the range $f \in [3.77, 11.40]$ appears a rotary oscillation, described by $x = A_0 + A_1 \cos\theta_1 \pm \omega t$. The terms $\omega t$ and $-\omega t$ correspond to rotations in the positive and negative directions, respectively. We can show that these are the only rotary oscillations in the case $\lambda = 0.1$ and $\omega = 2$. Figs.6 and 7 show typical structures in the period-tripled and modulated rotational state, respectively. The power spectrum in Fig.7 is obtained from $x(t)$ with -$\omega t$ subtracted. They can coexist with each other, and with the normal or even with the symmetry-broken state. Fig.8 presents an over-view, based on the analysis in §3. Two closed loops for $f \in [3.16, 5.97]$ correspond, respectively, to $A_1$ and $A_{1/3}$ in the period-tripled state, which means that this state consists of two branches. Linear analysis shows that the lower branch of loop $A_{1/3}$ and the upper branch of loop $A_1$ correspond to a locally stable state, while other branches to an unstable one. On the other hand, two closed loops for $f \in [3.77, 11.40]$ represent $A_0$ in the rotary regime, with the upper and lower loop corresponding to negative and positive rotations, respectively. The upper branch of the upper loop together with the lower branch of the lower loop corresponds to unstable states. Fig.9 is the enlargement of

Fig.8, and emphasizes the closed loops. Marks • and × on the loops are the results of the numerical integrations.

**§3. The analytic integrations.** Analysis in this section is based on the lowest approximation, and it should be noted that quantitative result change slightly, if higher order terms are included. We describe the normal state by the trial function

$$x = A_1 \cos\theta_1\,, \quad \theta_1 = \omega t - \alpha_1\,, \quad A_1 > 0\,, \quad 0 < \alpha_1 < \pi. \tag{3.1}$$

Substituting in (2.1) and ignoring all higher harmonics, we have

$$2\mathrm{J}_1(A_1) - \omega^2 A_1 = f\cos\alpha_1\,; \quad 2\lambda\omega A_1 = f\sin\alpha_1,$$

which leads to

$$\{2\mathrm{J}_1(A_1) - \omega^2 A_1\}^2 + (2\lambda\omega A_1)^2 = f^2\,; \quad \tan\alpha_1 = \frac{2\lambda\omega A_1}{2\mathrm{J}_1(A_1) - \omega^2 A_1}. \tag{3.2}$$

To study the local stability of the normal state, we add to the trial function an infinitesimal disturbance $\delta x$. The linearized equation for $\delta x$ then takes the form

$$\Big\{\mathrm{D}^2 + 2\lambda\mathrm{D} + \sum_{n=-\infty}^{\infty}(-1)^n \mathrm{J}_{2n}(A_1)\exp(2in\theta_1)\Big\}\delta x = 0. \tag{3.3}$$

We expand $\delta x$ in the Fourier series:

$$\delta x = \sum_{m=-\infty}^{\infty} \delta a_m \exp(im\theta_1)\,, \quad \delta a_{-m} = \delta a_m^*.$$

Substitution in (3.3) yields

$$\{\mathrm{D}^2 + 2(\lambda + i\omega)\mathrm{D} + 2i\lambda m\omega - m^2\omega^2\}\delta a_m - \sum_{n=-\infty}^{\infty} \mathrm{J}_{2n}(A_1)\delta a_{m-2n} = 0. \tag{3.4}$$

To see the stability of the fundamental mode, we put $m = 1$ to obtain

$$\{\mathrm{D}^2 + 2(\lambda + i\omega)\mathrm{D} + 2i\lambda\omega - \omega^2 + \mathrm{J}_0(A_1)\}\delta a_1 - \mathrm{J}_2(A_1)\delta a_{-1} = -\mathrm{J}_4(A_1)\delta a_{-3} + \mathrm{J}_2(A_1)\delta a_3 + \cdots.$$

Coupling with higher harmonics are shown to be negligible, and therefore

$$\{\mathrm{D}^2 + 2(\lambda + i\omega)\mathrm{D} + 2i\lambda\omega - \omega^2 + \mathrm{J}_0(A_1)\}\delta a_1 - \mathrm{J}_2(A_1)\delta a_{-1} = 0.$$

This is a basic equation of parametric resonance,[7] and for the normal state to be stable, resonance must not occur. This condition is written as $| 2i\lambda\omega - \omega^2 + \mathrm{J}_0(A_1) |^2 > \mathrm{J}_2^2(A_1)$, which is satisfied when $\omega \geq 2$. To study the stability of the normal state with respect to the dc disturbance $\delta a_0$, we put $m = 0$ in (3.4) to obtain

$$\{\mathrm{D}^2 + 2\lambda\mathrm{D} + \mathrm{J}_0(A_1)\}\delta a_0 = \mathrm{J}_2(A_1)(\delta a_2 + \delta_{-2}) + \cdots .$$

If we ignore even harmonics, $\delta a_0$ amplifies when $\mathrm{J}_0(A_1) < 0$, and a symmetry-breaking occurs. The critical amplitude in the lowest approximation is thus the first zero of $\mathrm{J}_0(A_1)$, and $f_c$ is given by (3.2) with $A_1$ replaced by $A_z$.

The lowest order trial function describing a symmetry-broken state is $x = A_0 + A_1 \cos\theta_1$. Substituting in (2.1), and ignoring all higher harmonics, we obtain

$$\sin A_0 \mathrm{J}_0(A_1) = 0\,; \quad 2\mathrm{J}_1(A_1)\cos A_0 - \omega^2 A_1 = f\cos\alpha_1\,; \quad 2\lambda\omega A_1 = f\sin\alpha_1 . \tag{3.5}$$

The first equation shows that, since $A_0$ is non-vanishing after symmetry is broken, $A_1$ must take the fixed value $A_z$. It follows from the remaining two equations that

$$\cos A_0 = \frac{\omega^2 A_0 \mp \{f^2 - (2\lambda\omega A_z)^2\}^{1/2}}{2\mathrm{J}_1(A_1)}, \qquad f > f_c .$$

Note that two solutions exist for $A_0$ differing only in sign. It can be easily shown that, when $A_0$ reaches $\pi$, $A_1$ increases as $f$ increases, until it arrives at the second zero of $\mathrm{J}_0(A_1)$.

We next consider the period-tripled state, and write the trial function in the form

$$x = A_1\cos\theta_1 + A_{1/3}\cos(\theta_{1/3} - \alpha_{1/3}).$$

Substituting in (2.1) and ignoring all higher harmonics, we find the following four equations:

$$-\omega^2 A_1 + 2\mathrm{J}_0(A_{1/3})\mathrm{J}_1(A_1) = f\cos\alpha_1\,; \quad (2\lambda\omega/3)A_{1/3} - 2\mathrm{J}_1(A_1)\mathrm{J}_2(A_{1/3})\sin\alpha_{1/3},$$

$$2\lambda\omega A_1 = f\sin\alpha_1\,; \quad 2\mathrm{J}_0(A_1)\mathrm{J}_1(A_1) - (\omega^2/9)A_{1/3} = 2\mathrm{J}_1(A_1)\mathrm{J}_2(A_{1/3})\cos\alpha_{1/3}.$$

Closed loops in Fig.8 are based on these formulae. The local stability can be studied by substituting in (2.1) the trial function

$$x = A_1\cos\theta_1 + A_{1/3}\cos\left(\theta_{1/3} - \alpha_{1/3}\right) + \{\delta a_1 \exp(i\theta_1) + \delta a_{1/3}\exp\left(i\theta_1/3\right) + \text{c.c.}\},$$

and linearize it with respect to the disturbance. The stable branches in Fig.8 have been identified with the aid of the stability analysis, but we shall not go into further detail.

We finally study the rotary oscillations of the pendulum. The analysis is based on the perturbation expansion method of Pederson et al.[8] The trial function is taken to be

$$x = A_0 + A_1 \cos\theta_1 \pm \omega t\,, \quad \theta_1 = \omega t - \alpha_1\,, \quad 0 < \alpha_1 < \pi$$

with the dual sign discriminating the sense of the rotation. We first consider the rotation in the positive direction. Substituting in (2.1) the trial function with the plus sign, and ignoring higher harmonics, we obtain the three equations:

$$2\lambda\omega A_1 + \cos(\beta_+)\mathrm{J}_1(A_1) = 0\,; \quad -\omega^2 A_1 + \sin\beta_+)\{\mathrm{J}_0(A_1) - \mathrm{J}_2(A_1)\} = f\cos\alpha_1,$$

$$-2\lambda\omega A_1 + \cos(\beta_+)\{\mathrm{J}_0(A_1) + \mathrm{J}_2(A_1)\} = -f\sin\alpha_1,$$

where $\beta_+ = A_0 + \alpha_1$. Obviously, the rotary regime never exists if $2\lambda\omega$ exceeds the maximum value of $\mid \mathrm{J}_1(A_1) \mid$, or if $\lambda\omega > 0.291$. The closed loops together with the isolated branch in the range $f \in [3.77, 11.40]$ in Fig.8 are based on these formulae. When the rotation is in the negative direction, the analysis is completely the same, except that $\beta_+$ is replaced by $\beta_- = A_0 - \alpha_1$. We shall not go into detail of the stability analysis.

**§4. Summary and discussion.** The dynamical structures of the driven pendulum in the pre-chaotic phase have been studied, and it has been shown that absence of chaos leads for its substitute to an inversion of the pendulum. It has also been shown that, for intermediate values of $f$, four stationary motions (period-single and period-tripled state, and rotary oscillations in the positive and negative direction) coexist. It is remarkable that most quantitative features of the dynamics can be explained analytically in the lowest approximation, and that non-chaotic motions admitting such a simple quantitative analysis exist in the vicinity of the chaotic phase.

## References


1 ) K. Tomita, Phys. Rep. **86** (1982), 114, and references therein.

2 ) H. G. Schuster, *Deterministic Chaos.* (VCH, Weinheim, Germany, 1989).

3 ) T. Geisel and J. Nierwetberg, Phys. Rev. Lett. **48** (1982), 7.

4 ) S. Grossmann and H. Fuzisaka, Phys. Rev. **26A** (1982), 1779.

5 ) T. Geisel and S. Thomae, Phys. Rev. Lett. **52** (1984), 1936.

6 ) R. C. Kautz, J. Appl. Phys. **52** (1981), 624.

7 ) N. Takimoto and H. Yamashida, Physica **26D** (1987), 251.

8 ) N. I. Pederson et al., J. Low Temp. Phys. **38** (1080), 1.